

Plasma Diagnostics of the $\mu 10$ ECR Ion Thruster Using Optical Fiber Probes

IEPC-2013-270

*Presented at the 33rd International Electric Propulsion Conference,
The George Washington University • Washington, D.C. • USA
October 6 – 10, 2013*

Ryudo Tsukizaki¹
Japan Aerospace Exploration Agency, Sagamihara, Kanagawa, 252-5210, Japan

Toshiyuki Ise² and Hiroyuki Koizumi³
The University of Tokyo, Bunkyo-ku, Tokyo, 113-8656, Japan

Hiroyoshi Togo⁴
Nippon Telegraph and Telephone Corporation, Atsugi, Kanagawa, 243-0198, Japan

and

Kazutaka Nishiyama⁵ and Hitoshi Kuninaka⁶
Japan Aerospace Exploration Agency, Sagamihara, Kanagawa, 252-5210, Japan

In order to reveal the physical processes taking place within the ECR ion thruster “ $\mu 10$ ”, internal plasma diagnosis is indispensable. However, the ability of metallic probes to access microwave plasmas biased at a high voltage is limited from the standpoints of the disturbance created in the electric field and electrical isolation. This study demonstrates two kinds of plasma parameter measurements using optical fibers. Firstly, an optical fiber probe is a single-mode optical fiber. It is used to guide laser into the discharge chamber in the measurement of Xe I by the laser absorption spectroscopy. The other is an EO probe to measure the electric field of microwaves. From the both results, it can be deduced that there is plasma in the waveguide in the propellant injection from a waveguide. To improve the thrust force, it is important to suppress the electron in the waveguide.

I. Introduction

The electron cyclotron resonance (ECR) ion thruster “ $\mu 10$ ”¹ was first demonstrated in space onboard the Japanese asteroid explorer HAYABUSA, which was launched on May 9, 2003 and returned to Earth on June 13, 2010. Based on the success of the mission, the $\mu 10$ thruster is scheduled to be used in the HAYABUSA2 spacecraft bound for another asteroid, and to be commercialized for use in geosynchronous satellites. For these spacecraft, several improvements were made to the $\mu 10$ thruster.²

¹ Assistant Professor, Department of Space Flight Systems, Institute of Space and Astronautical Science, ryudo@ep.isas.jaxa.jp

² Graduate Student, Department of Aeronautics and Astronautics, ise@ep.isas.jaxa.jp

³ Associate Professor, Research Center for Advanced Science and Technology, koizumi@al.t.u-tokyo.ac.jp

⁴ Senior Research Engineer, Microsystem Integration Laboratories, togo.hiroyoshi@lab.ntt.co.jp

⁵ Associate Professor, Department of Space Flight Systems, Institute of Space and Astronautical Science, nishiyama@ep.isas.jaxa.jp

⁶ Program Director, Lunar and Planetary Exploration Program Group, kuninaka@ep.isas.jaxa.jp

However, there was no room to increase the ion beam current by increasing the microwave power.³ In addition, two modes—low-beam current mode and high-beam current mode—have been identified in $\mu 10$ operation.² In order to make further improvements to the $\mu 10$ thruster and to clarify the two modes, internal plasma diagnoses with spatial resolution in the ion beam acceleration state is necessary. The Langmuir probe is a well-developed technique used to measure local plasma, although it disturbs the microwave electromagnetic field. Optical techniques such as laser absorption spectroscopy yield information integrated with respect to the line of sight without spatial resolution in depth, which may be improved by means of an Abel conversion using a great deal of tomography data.

Plasma states in the plasma source under beam acceleration and at the time of plasma ignition are different, even under conditions of the same microwave power and gas flow rate. Beam acceleration ejects gas to the outside so that the gas pressure in the plasma source is lower than that at the time of plasma ignition. The best way to investigate the physics of ion engines is to measure plasma under beam acceleration, although ignited plasma at a reduced gas flow rate might be used to simulate the plasma state under beam acceleration.⁴

In this paper, two novel methods are conducted in order to measure plasma parameters. One is the number density distribution measurement of Xe I 828.01 nm in plasma using a slender optical fiber adopting laser absorption spectroscopy.⁵ The other is the microwave electric field measurement using a polarization-maintaining optical fiber attached with Electro-Optic (EO) element.⁶

Compared with metallic probes such as the Langmuir probe, the use of optical fibers has the following merits:

1. It creates little disturbance in the microwave electromagnetic field because it is a dielectric material.
2. It can be used in high-voltage plasma because it is an insulator.

As well as the metallic probes, the optical fiber probe can endure high temperature and realize nondestructive monitoring of plasma measurements inside plasma sources by insertion through a grid aperture in an ion accelerating state. Moreover the optical fiber can be easily traversed, which gives us information on local plasma. This paper will clarify the difference of two modes and the mechanism of the improvements of the thrust force by the measurements.

II. Experiment

A. The ECR $\mu 10$ Ion Thruster

A schematic of the ECR ion thruster $\mu 10$ is shown in Fig. 1. The ECR ion thruster $\mu 10$ basically consists of a waveguide, a discharge chamber, a three-grid system and a neutralizer. Additionally, there is a microwave antenna and a propellant inlet at one end of the waveguide. The other end of the waveguide is connected to the discharge chamber (right side in Fig. 1) A microwave with a frequency of 4.25 GHz is transmitted through the waveguide to the discharge chamber. In the discharge chamber there are two rings of samarium-cobalt magnets. A propellant, Xenon, is injected via the inlets and flows into the discharge chamber. In the discharge chamber, electrons are accelerated by a mirror magnetic field and ECR heating. By subsequent electron-neutral and electron-ion collisions, ECR plasma is formed. The thrust force of the $\mu 10$ thruster was improved by changing the propellant injection location. In the flight model of HAYABUSA, it located at the end of the waveguide. In the improved model, it is also opened in the discharge chamber, and the propellant is distributed at the ratio of 1 to 2 between the waveguide inlet and the discharge chamber inlets. A summary of the operational conditions is shown in Table 1.

Table 1. The Specifications of the improved $\mu 10$.

Beam diameter (mm)	105
Microwave frequency (GHz)	4.25
Screen voltage (V)	1500
Accelerator voltage (V)	-350
Decelerator and neutralizer voltage (V)	~ -30
Thrust force (mN)	10.1
Beam current (mA)	170
Specific impulse (sec)	3160
Mass utilization efficiency (%)	85
Ion production cost (eV)	200
Nominal Xenon flow rate (scm)	2.70
Microwave power (W)	34

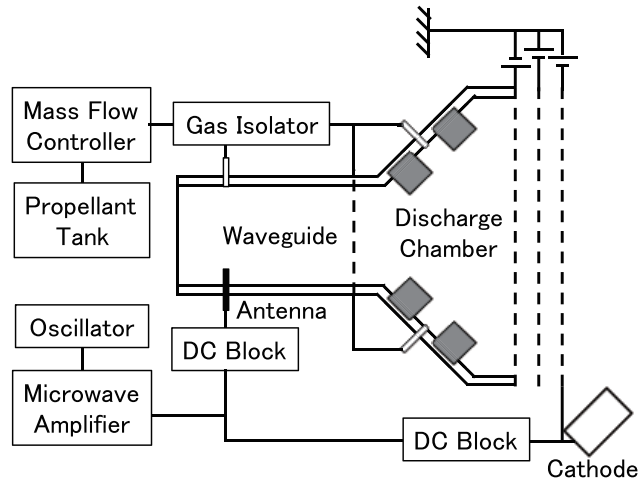


Fig. 1. The schematic of the $\mu 10$ microwave ion thruster.

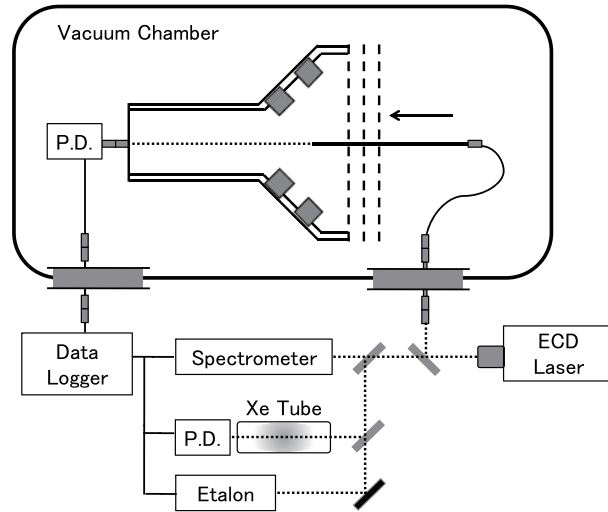


Fig. 2. The experimental setup for laser absorption spectroscopy. P.D. stands for “photo detector,” and ECD for “external cavity diode.”

B. Number density distribution measurement of Xe I 828.01 nm using optical fiber probe

The experimental setup for laser absorption spectroscopy is shown in Fig. 2. A probe on a highly accurate linear stage is automatically inserted in the plasma source through the center aperture of the grid system. At the end of the waveguide is a condenser lens, which is connected to a photo detector via a multi-mode optical fiber inside a vacuum chamber. A data logger records the signal from the photo detector and etalon. As the fiber moves into the plasma source, the length of the laser path becomes shorter, which changes the area of the absorption spectra. The number density distribution is obtained by differentiating the neighboring absorption areas. The experimental conditions are listed in Table 2.

Propellant flow rates (sccm)	WG 1, 2, 3 DC 2, 3, 4
Measurement points (cm)	0- -14
Sweeping frequency of wavelength (Hz)	50
Number of samples	100

C. Electric field measurement using EO probe

The experimental setup for the electric field measurements is shown in Fig. 3. In the vacuum chamber, the EO probe is installed in a silica glass tube of 3 mm diameter, which is mounted on a linear stage and a rotary stage positioned by stepping motors. The probe is remotely inserted in the discharge chamber through the center aperture of the grid system. The measurement interval is 1 cm. The rotational angle is adjusted so that the measurement direction of the EO probe is parallel to the longitudinal direction of the dipole antenna, where the maximum electric field is detected.

Outside the vacuum chamber, a laser diode (LD), a polarization controller, a photodiode (PD), and a spectrum analyzer are set. The polarization controller comprises a polarizer, a circulator, half and quarter-wave plates (WPs), and an analyzer. The light wave emitted from the LD is polarized linearly by the polarizer, inputted into the PMF, and reaches the tip of the probe through the circulator. The light wave makes a round-trip pass through the EO crystal via reflection by the dielectric reflector and the polarization of the lightwave changes in proportion to the microwave electric field along the measurement direction. The polarization-changed light is returned to the polarization controller and converted to linearly polarized light with the analyzer. That is, the lightwave is intensity-modulated by the microwave electric field. The intensity-modulated light is detected and converted to an electric signal by the PD. The amplitude and phase of the electric signal are proportional to those of the microwave electric field, and the frequency of the electric signal is the same with that of the microwave electric field. As a microwave signal is input to the Ion Thruster at a frequency of 4.25 GHz, the spectrum analyzer displays the spectrum with the intensity proportional to that of the measured microwave electric field at a frequency of 4.25 GHz.

The EO probe is calibrated using a rectangular waveguide with a cross section of $2.0 \times 4.0 \text{ cm}^2$. The waveguide is connected by a coaxial-waveguide converter at one end and terminated by a dummy load at the other end. The waveguide produces a traveling-wave. The EO probe is set on the center axis of the waveguide where the electric field intensity is maximal. The output of the EO probe displayed on the spectrum analyzer is calibrated by the theoretical electric field intensity in the waveguide at a known microwave power.

A schematic of the cooling system is shown in Fig. 4. The cooling system consists of a silica glass tube of 3 mm diameter, a Pyrex glass tube of 1.8 mm diameter, a PTFE tube for piping of 1/4 inch diameter, and a fine Teflon tube to introduce cooling air. The EO probe is set inside the Pyrex glass tube, which maintains the probe in a horizontal position and prevents its vibration by high-pressure air. One end of the 1/4-inch PTFE tube is connected to the silica glass tube and the other end is led to the outside of the vacuum chamber through a feed through of a flange. The 1/4-inch PTFE tube has a length of 1.5 m. One end of the fine PTFE tube is inserted in the silica glass tube and the other end is connected to a high-pressure air source in atmosphere. An optical fiber attached to the EO crystal leads to the outside of the vacuum chamber through the 1/4-inch PTFE tube and is connected to the optical devices and the spectrum analyzer. High-pressure air from the air source is introduced into the glass tube through the fine PTFE tube and cools the EO probe. Then, cooling gas is exhausted to the outside of the chamber through the 1/4-inch PTFE tube. The EO probe inside the Pyrex glass tube fixed in the silica glass tube can be adjusted in position and sensitive direction by a linear and a rotary stage. In addition, because the accelerated plasma from the ion thruster directly hits and heats the tube coupling and the rotary stage, a beam barrier is set between the ion source and the cooling system. The cooling system keeps the air temperature around the EO probe at around 25 degrees Celsius even under beam acceleration, allowing measurement of the electric field in the accelerated plasma with the same accuracy as in atmosphere.

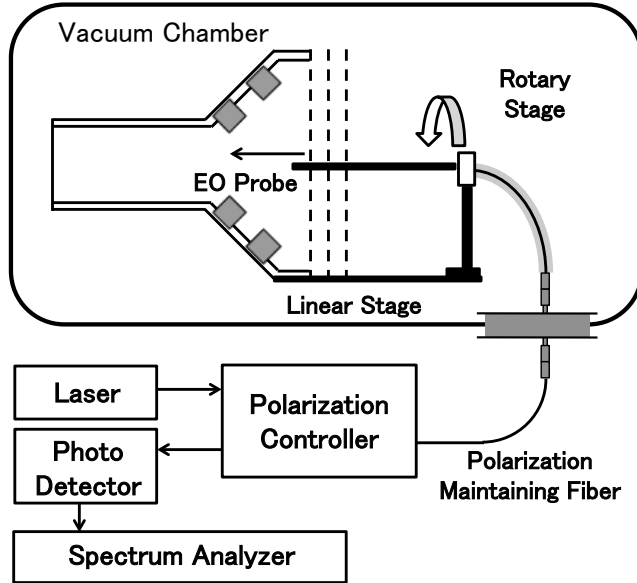


Fig. 3. The experimental setup for electric field measurement along the centerline of the plasma source.

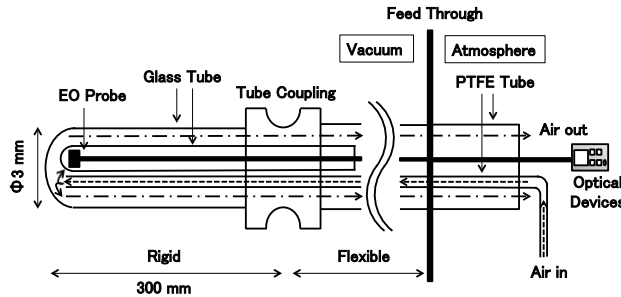


Fig. 4. The schematic of cooling system for electric field measurement in the accelerated plasma. The air temperature around the EO probe is kept at around 25 degrees Celsius.

III. Experimental results and discussion

A. Number density measurement of Xe I 828.01 nm using optical fiber

The number density distribution of Xe I 828.01 nm is shown in Fig. 5. In the measurement of Xe I 828.01 nm, the highest absorption was less than 2%. Compared with Xe I 823.16 nm which has about 90% of absorption,⁴⁾ the accuracy of zero line significantly affects the result of the number density distribution, which resulted in the decrease of its spatial resolution from 1 cm to 2 cm. Even in the 2 cm spatial resolution, the error bar for the zero line is bigger than the measurement of Xe I 823.16 nm. Moreover, at the propellant flow rate of 1.00 sccm from the waveguide inlet and 2.00 sccm from the discharge chamber inlets, the absorption was less than 0.1%. And it was impossible to detect with the current experimental setup. When the propellant was injected from the waveguide inlet, the highest values were recorded in the waveguide, which were $7.9 \times 10^{15} \text{ m}^{-3}$ at the propellant flow rate of 3.00 sccm and $1.3 \times 10^{16} \text{ m}^{-3}$ at 4.00 sccm. In the case where propellant was injected from the discharge chamber inlets, there existed the maximum number densities in the discharge chamber. At the propellant flow rates of 3.00 sccm and 4.00 sccm, the maximum values are $6.8 \times 10^{15} \text{ m}^{-3}$ and $1.5 \times 10^{16} \text{ m}^{-3}$ respectively in the discharge chamber. The lifetime of Xe I 828.01 nm is reported to be 1-10 μs ,^{7,8} and the excited particle is estimated to be movable about 0.5-5 mm under the assumption that the density of neutral particles is 10^{19} m^{-3} and that the thermal velocity is 1000 K. The particles are excited and quickly decayed at almost the same location. Therefore, the peak of Xe I 828.01 nm in the waveguide indicates that there exists the peak of electron density. The location from 7 cm to 9 cm from the screen grid is matched with the anti-node of the stationary microwave. However, electrons are not accelerated to 8.44 eV only by microwaves in the waveguide. It is therefore assumed that the electrons come from the ECR region in the discharge chamber along with the magnetic lines.

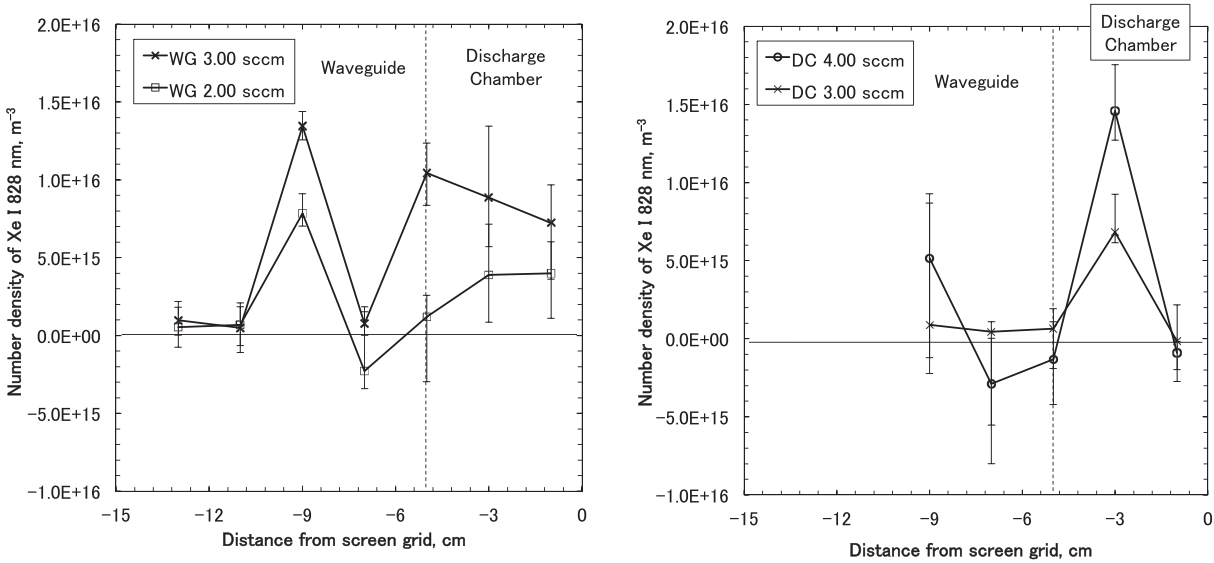


Fig. 5. The distribution of number densities of Xe I 828.01 nm in the $\mu 10$ thruster. The left figure shows the distribution at the propellant flow rates of 1.00, 2.00, and 3.00 sccm from the waveguide inlet, and the right figure shows the distribution at the propellant flow rates of 3.00 and 4.00 sccm from the discharge chamber inlets. At the propellant flow rate of 2.00 sccm from the discharge chamber inlets, no absorption was recorded. The error bar derives from the accuracy of the zero line of the absorption spectrum.

B. Electric field measurement using EO probe

The oscillating electric field distribution parallel to the dipole antenna along the centerline of the plasma source was measured with respect to the propellant flow rate, shown in Fig. 6. This measurement was conducted under beam acceleration. In the accelerated plasma source, the cooling system kept the air temperature around the EO probe at around 25 degrees Celsius, so the measurement accuracy was the same as in atmosphere. The distribution of the electric field with plasma is completely different from that without plasma (0 sccm).

The above figure of Fig. 6 shows the result when the propellant was injected from the waveguide inlet. At a propellant flow rate of 1.00 sccm, before the beam current saturation, the electric field intensity is relatively low compared with that for other flow rates, especially in the waveguide. At propellant flow rates more than 2.00 sccm from the waveguide inlet, after the beam current saturation, the electric field intensity in the waveguide saturates.

The bottom figure shows the result when the propellant was injected from the discharge chamber inlets. By the propellant flow rates increased to 2.4 sccm, the intensity of electric field was suppressed in the waveguide. This result indicates the propellant injection from the discharge chamber inlets is effective not to produce the peak of the electric field of the microwave in the waveguide.

Fig. 6 shows that there are clear differences in the electric field distribution before and after the beam current saturation. This result indicates that the electric field distribution inside the thruster is related to the beam current and changes in the electric field distribution may cause the beam current to stall. The electric field intensity at the centerline cannot be directly connected to the whole beam current of the discharge chamber. In order to examine the mechanism further, we need to measure the overall profile of the electric field inside the discharge chamber. In particular, the electric field intensity at the ECR area plays a critical role in electron heating and its measurement is very important for understanding the physics of the microwave discharge plasma. However, such a detailed measurement is beyond the scope of this study which is to verify a new method to measure microwave discharge plasma.

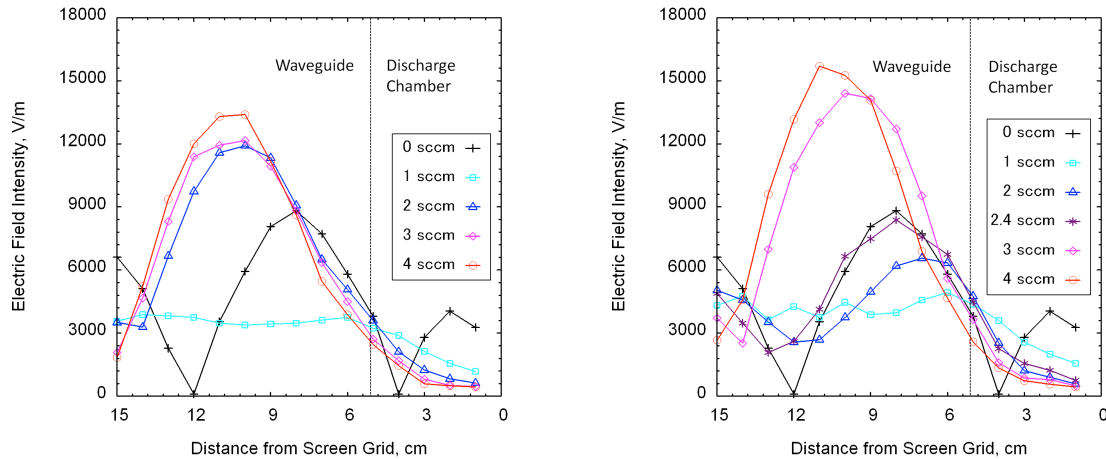


Fig. 6. The electric field distribution oscillating parallel to the dipole antenna along the centerline of the ion thruster. The left figure shows the result when the propellant was injected from the waveguide inlet, the right shows when the propellant was injected from the discharge chamber inlets.

IV. Conclusion

In this study, the two plasma parameter measurements of the microwave ion thruster $\mu 10$ were conducted utilizing optical fiber probes. The measurements made it possible to measure plasma parameters of microwave ion sources under ion beam acceleration.

Firstly, it was turned out that the non-metastable Xe I 828.01 nm was distributed with a $10^{15-16} \text{ m}^{-3}$ order of magnitude of number densities. The highest densities were recorded in the waveguide when the propellant was injected from the waveguide inlet. It implied that the excitation collisions of electrons with neutral particles occurred most at the anti-node of microwave in the waveguide.

Secondly, the microwave electric field measurement with an EO probe revealed that the intensity of the electric field in the waveguide abnormally increased at the propellant flow rate of 2.00 sccm from the waveguide inlet. Once it happened, the microwave started reflecting, which resulted in the saturation of the beam current.

Regarding the above two plasma diagnoses, it can be concluded that the electron density in the waveguide possibly reached the cut-off density at the propellant flow rate of over 2.00 sccm from the waveguide inlet. As a consequence, to improve the thrust force of the $\mu 10$ thruster, it is highly important to suppress the plasma in the waveguide.

Acknowledgments

This work is financially supported by grant-in-aid 25•444 for JSPS fellows.

References

- ¹Kuninaka, H.: Development and Demonstration of a Cathode-less Electron Cyclotron Resonance Ion Thruster, Journal of Propulsion and Power, Vol. 14, No. 6, pp.1022-1026, 1998.
- ²Tsukizaki, R., Koizumi, H., Hosoda, S., Nishiyama, K., Kuninaka, H.: Improvement of the Thrust Force of the ECR Ion Thruster $\mu 10$, Trans. JSASS Space Tech. Japan, Vol. 8, pp. Pb_67-Pb_72, 2010
- ³Nishiyama, K., Hosoda, S., Usui, M., Tsukizaki, R., Hayashi, H., Shimizu, Y., Kuninaka, H.: Feasibility Study on Performance Enhancement Options for the ECR Ion Thruster $\mu 10$, Trans. JSASS Space Tech. Japan, Vol. 7, pp. Pb_113-Pb_118, 2009.
- ⁴Funaki, I., Kuninaka, H., Shimizu, K., Toki: Plasma Diagnostics and numerical modeling of a microwave ion engine, 34th AIAA/ASME/SAE/ASEE Joint Propulsion Conference & Exhibit, Cleveland, Ohio, USA, July 13-15, 1998.
- ⁵Tsukizaki, R., Koizumi, H., Nishiyama, K., and Kuninaka, H.: Measurement of axial neutral density profiles in a microwave discharge ion thruster by laser absorption spectroscopy with optical fiber probes, Rev. Sci. Instrum., Vol. 82, pp. 123103-1-6, 2011.

⁶Ise, T., Tsukizaki, R., Togo, H., Koizumi, H., and Kuninaka, H.: Electric field measurement in microwave discharge ion thruster with electro-optic probe, *Rev. Sci. Instrum.*, Vol. 83, pp. 124702-1-6, 2012.

⁷Anderson, H. M., Bergeson, S. D., and Lawler, J. E.: Xenon 147-nm Resonance f Value and Trapped Decay Rates, *Physical Review A*, Vol. 51, No. 1, pp. 211-217, 1995.

⁸Walhout, M., and Rolston, L. S., Analytical Formula for Radiation Trapping with Partial Frequency Redistribution, *Journal of Physics D*, Vol. 31, No. 22, pp. 3235-3242, 1998.